

# DEVELOPMENT OF SIMPLIFIED ANALYSIS CODES FOR 9-M DROP AND 1-M PUNCTURE TESTS FOR A RADIOACTIVE MATERIAL TRANSPORT CASK

K. Asada, M. Yamamoto  
Mitsubishi Heavy Industries, Ltd.  
Takasago Research & Development Center  
1-1, 2-chome, Niihama, Arai-cho  
Takasago 676, Japan

M. Ohashi, S. Hode, A. Higashino  
Mitsubishi Heavy Industries, Ltd.  
Kobe Shipyard & Engine Works  
1-1, 1-chome, Wadasaki-cho, Hyogo-ku  
Kobe 652, Japan

## ABSTRACT

The two simplified computer codes (CASH-II 7 CAPUC) usable for the design or safety analysis of a radioactive material transport cask have been developed. They can handily evaluate (1) the performance of the shock absorber(s) under the 9-m free drop accident condition and (2) the strength of the cask body under the 1-m puncture drop accident condition, respectively.

After outlining the theories, this paper describes the effectiveness of these codes by comparing their output results with the experimental data and other calculations.

## INTRODUCTION

A large package (see Fig. 1) for radioactive transport (hereafter called "cask") is regulatively required to maintain its integrity against the tests where it is dropped onto a rigid flat surface from a height of 9m, and then, as a puncture test, onto a 150 mm diameter mild steel bar from a height of 1 m. There are generally two methods to analyze its behaviors at the above tests. One is to use a sophisticated code (e.g. PISCES code, HONDO-II code, etc.) to analyze dynamic interactions against an impact, and the other is to use a simplified code to statically analyze such phenomena.

The method using the former is suitable for comparing experimental data with analytical results and for performing detail analyses, whereas the method using the latter is suitable for deciding the basic structure by performing parametric surveys.

As described above, in cask designing, it is very important not only to use a code to analyze dynamic interactions, but also to use appropriate codes for simple and quick analyses of the phenomena, therefore the following two simplified analyses codes have been developed by MHI:

1. A computer code to analyze the acceleration of a cask body and the displacement of its shock absorber(s) statically for the 9-m drop test (drop attitude: optional) -- CASH-II code
2. A computer code to analyze the acceleration and the displacement of a cask body statically for the 1-m puncture test (drop attitude: vertical) -- CAPUC code

## Background of Development

The cask has to maintain its integrity under the 9-m drop accident condition, so shock absorbers are to be

properly attached on the body so as to reduce the impact generated in the drop.

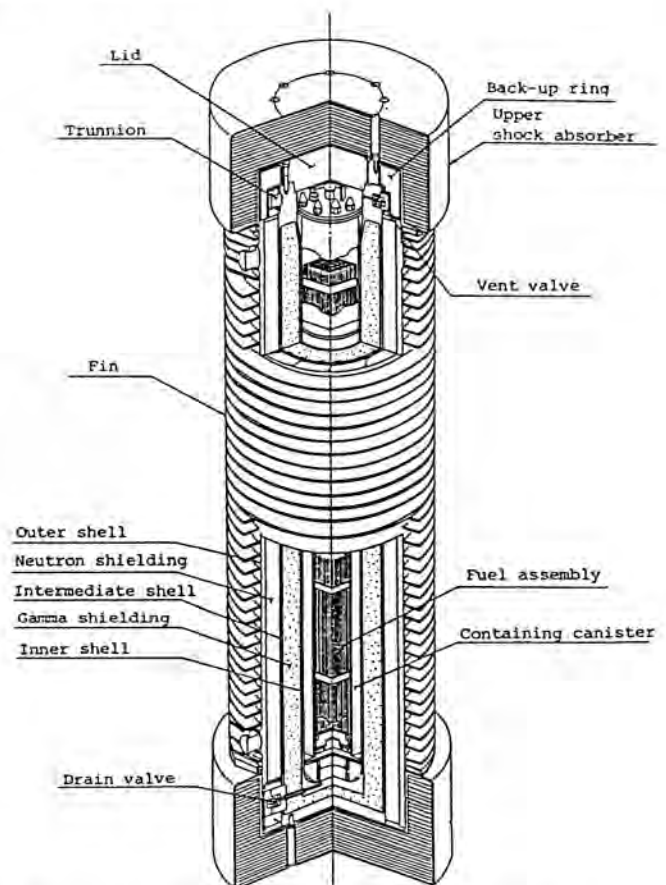


Fig. 1. Spent Fuel Transport Cask (Developed by MHI)

It is required to analyze the impact on the shock absorber in order to evaluate its effectiveness in the drop; besides the above, there is another important matter that the limitation of dimensions concerning handling and installation of the cask has to be satisfied.

In order to determine the appropriate dimensions and materials for the shock absorber in the stage of design, it is required to execute parametric surveys, that is to say, the following will be required for computer codes to evaluate the performance of the shock absorber:

1. Evaluation results can be obtained within a short time.
2. Cost of analysis is low.
3. Solution of high accuracy can be available.

Sophisticated codes (e.g., PISCES, HONDO-II) generally do not satisfy the requirements of the above 1) and 2), despite their satisfying the requirement 3), so we have developed CASH-II code which could satisfy all of the requirements cited above.

Theory

1. Drop attitudes

CASH-II code is capable of analyzing the cask behavior at the 9-m drop test for four attitudes (vertical, horizontal, corner and oblique) as shown in Fig. 2.

2. Outline of method (See Fig. 3)

CASH-II code is a program which evaluates statically, for each of the above drop attitudes, the cask body acceleration and shock absorber deformation to be caused by the drop from a 9-m height using the Uniaxial Displacement Method (UDM).

Conventionally, it has been a usual practice to use the Volumetric Displacement Method (VDM) for evaluation of a large three dimensional deformation. In VDM the absorption of drop energy is to be evaluated only by the volumetric quantity lost by the deformation of the shock absorber. This method is therefore considered as an effective means of evaluation provided the material can be dealt with under a constant compressive stress at any deformation. However, to assume the material properties in that way would be a bit problematic in view of the solution accuracy.

UDM, instead, will execute the evaluation under the assumption that the deformable domain consists of an assembly of many one-dimensional rod elements, and that all volume of the shock absorber can absorb the drop energy, so that the method makes a benefit of obtaining an accurate solution, though the analysis itself gets rather complicated compared with VDM.

3. Calculation model

In modeling a shock absorber in CASH-II code, it is assumed that the shock absorber consists of three species of wood (A, B and C) as shown in Fig. 4. In the figure, the symbols of I ~ IV indicate their analysis regions determined by the geometries of the cask and the shock absorber.

4. Theory

When the shock absorber deforms by a displacement  $\delta$  in a vertical drop, the impact load  $F_z(\delta)$ , and the dissipated energy  $E_z(\delta)$  are given by Eq. (1) and E. (2).

$$F_z(\delta) = k_1(S_{I\sigma I} + S_{II\sigma II}) + k_2 S_{III\sigma III} + k_3 S_{IV\sigma IV} \quad (1)$$

$$E_z(\delta) = \int_0^\delta F_z(\delta) d\delta \quad (2)$$

Where

- $k_1, k_2, k_3$  : constants ( $0 \leq k_i \leq 1$ ) determined by boundary conditons
- $\sigma_i (i=I-IV)$  : stress in the region  $i$  (function of  $\delta$ )
- $S_i (i=I-IV)$  : cross sectional area of the region  $i$
- $z$  : suffix for vertical drop

For evaluating the horizontal drop, the impact load  $F_x(\delta)$  and the dissipated energy  $E_x(\delta)$  can also be obtained by using equations similar to the above Eq. (1) and Eq. (2). (Where,  $x$  is a suffix for horizontal drop).

Now, including the effect of the wood grain (vener) angle and the material constant  $m$ , the stress of a wooden shock absorber can be written as follows:

$$\sigma_\alpha = \sigma_0 \cdot (\cos \alpha)^m + \sigma_{90} \cdot (\sin \alpha)^m \quad (3)$$

Where

$\sigma_0, \sigma_{90}, \sigma_\alpha$ : Stresses in the wood whose grain (vener) direction is parallel, perpendicular and angle degree to the drop direction, respectively.

As an example, in regard to the stress in the shock absorber made of fir plywood whose grain (vener) direction is 60 degree to the drop direction, a comparison between Eq. (3) and an experiment is shown in Fig. 5. From the comparisons like this, the value of  $m$  is determined.

As for the corner and oblique drops, the impact load and dissipated energy are difficult to determine exactly, because the boundary conditions of the analysis become complex compared with those of the vertical and horizontal drops. For this reason, we derive approximate equations (Eq. [4] and Eq. [5]) to analyze the impact load  $F_\theta(\delta)$  and dissipated energy  $E_\theta(\delta)$  for such drops, taking advantage of the wood stress-oblique angle relation given by Eq. (3).

$$F_\theta(\delta) = F_z(\delta_B \cos \theta) \cdot (\cos \theta)^{m-1} + F_x(\delta_B \sin \theta) \cdot (\sin \theta)^{m-1} \quad (4)$$

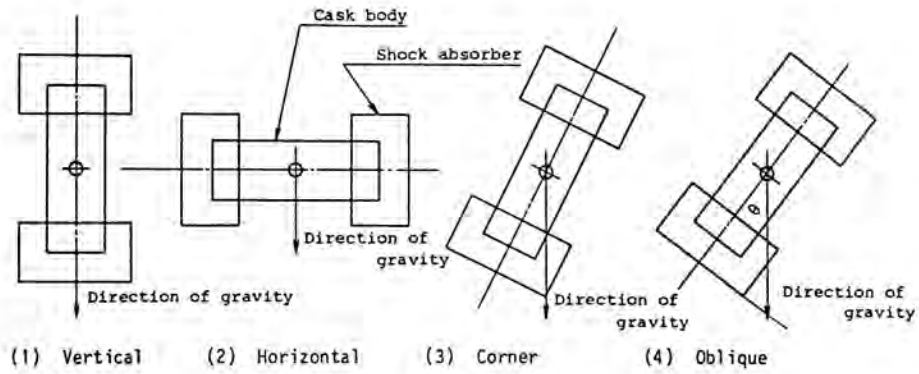


Fig. 2. Cask Attitude in 9-m Drop Test.

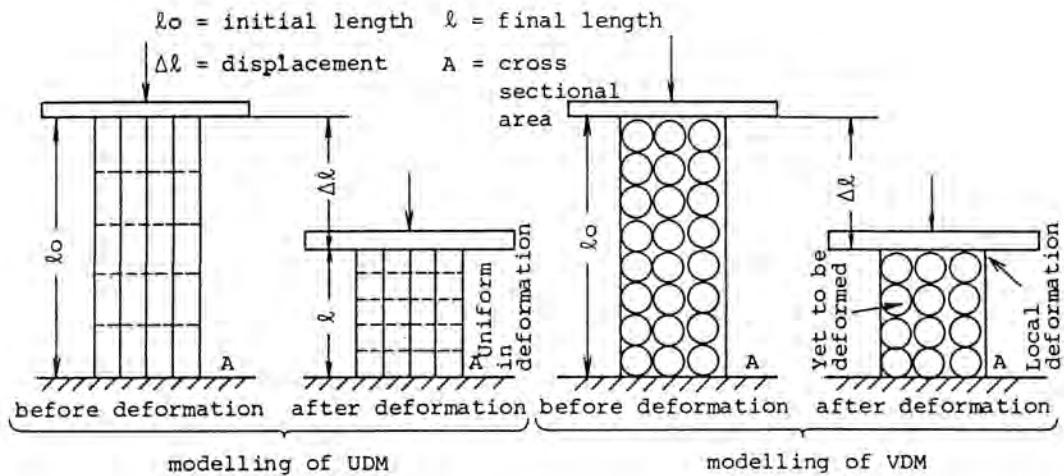


Fig. 3. UDM vs. VDM

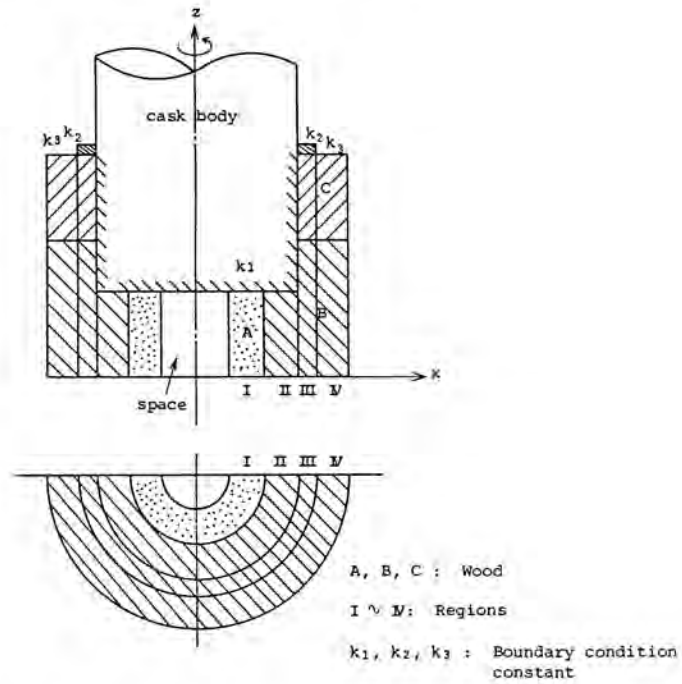


Fig. 4. Analysis Model of Shock Absorber (Vertical Drop).

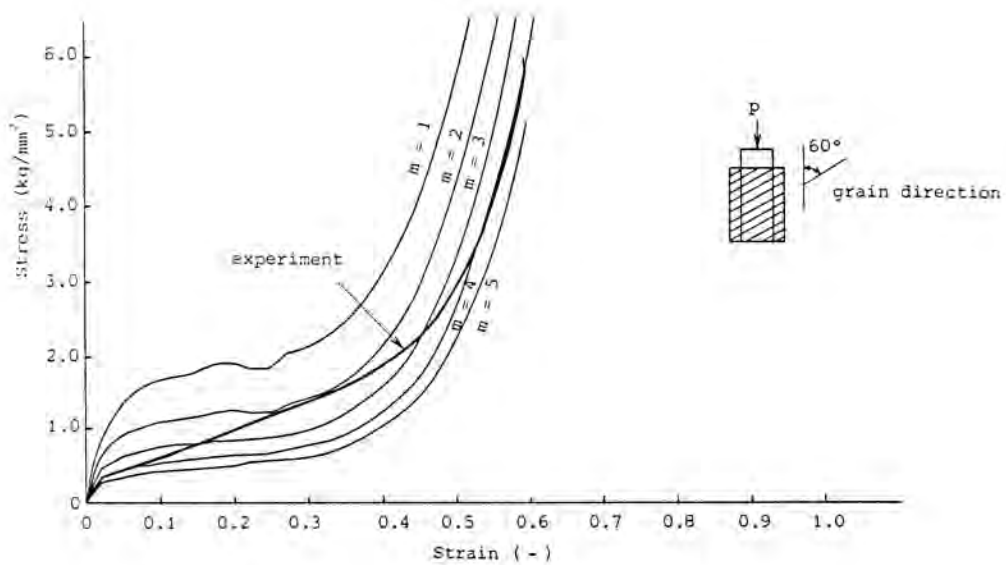


Fig. 5. Stress vs. Strain Diagram (Fir Plywood).

$$E_{\theta}(\delta_{\theta}) = E_z(\delta_{\theta} \cos \theta) \cdot (\cos \theta)^{m-2} + E_x(\delta_{\theta} \sin \theta) \cdot (\sin \theta)^{m-2} \quad (5)$$

Where

$\delta_{\theta}$ : Oblique displacement.

$\theta$ : Oblique angle.

$F_z(\delta_{\theta} \cos \theta), F_x(\delta_{\theta} \sin \theta)$  : Vertical and horizontal impact loads, respectively.

$E_z(\delta_{\theta} \cos \theta), E_x(\delta_{\theta} \sin \theta)$  : Vertical and horizontal dissipated energies, respectively.

Therefore, when a cask whose weight is  $W$  is dropped from a height of  $H$  with an oblique angle of  $\theta$  the maximum displacement of the shock absorber  $\delta_{\theta}^*$  and the maximum acceleration of the cask body  $G^*$  are given by Eq. (6) and Eq. (7) by using Eq. (5) and Eq. (4), respectively.

$$E_{\theta}(\delta_{\theta}^*) = \epsilon \cdot W \cdot H \quad (6)$$

$$G^* = F_{\theta}(\delta_{\theta}^*)/W \quad (7)$$

Where

$\epsilon$ : Ratio of the energy absorbed in the primary impact to the total energy absorbed in the primary and secondary impacts.

#### Comparison between CASH-II Calculation and Experiment

Figure 6 shows a CASH-II code output example as to the relations between the acceleration and deformation and also between the acceleration and drop energy (cask weight  $\times$  drop height) which were calculated for the vertical drops of the type-II spent fuel transport cask developed by MHI (see Table I).

In regard to the Type-I cask, the relation among the oblique angle, the acceleration and the displacement in the primary impact is shown in Fig. 7.

And some example comparisons among the results obtained from CASH-II code, experiments and sophisticated codes are shown in Table II.

From the studies as exemplified in Table II, the results of CASH-II code nearly agree with the experimental data and those of the sophisticated code as well. However, the acceleration values of CASH-II code analyses are generally less than those of experiments and sophisticated code analyses, therefore, in applying the code to actual full scale design, the values are used for proper/conservative estimations by multiplying a constant value of 1.2 as a dynamic factor including, if applicable, scale effects.

## CAPUC CODE

### Background of Development

As mentioned in INTRODUCTION, it is required for the cask to maintain its integrity against the 1-m puncture test. For this reason, the cask wall (i.e., shell, bottom and lid) is desired to be thick. However, it would be required to make the wall thicknesses thinned as much as possible, because a severe weight restriction is usually imposed on the cask design. Especially, the lid thickness is important for the seal integrity. So, the optimum design of the wall thicknesses is required.

Conventionally, the evaluation of the 1-m puncture test has been executed based on real experiments or sophisticated codes. However, if the former is taken, the range of the results' application to other cask designs will be limited, and if the latter is taken, much calculation time will be required.

In order to meet the above requirements, CAPUC code has been developed, thus facilitating the evaluation of the 1-m vertical drop puncture test.

### Theory

#### 1. Outline of method

When the cask is dropped onto the mild steel bar in the 1-m puncture test, the kinetic energy of the cask is absorbed into deformation of both the cask body and the mild steel bar, provided the puncture does not take place. The deformation generated on the cask body can be evaluated based on the fact that the loads generated on the cask and the mild steel bar are equal to each other. In this evaluation, the plastic theory of bending of a circular plate having a multilayer construction (e.g., steel-lead-steel) is used, which has been developed by extending the Onat's theory (1).

#### 2. Theory

When a distributed load is applied to a three-layer circular plate rigidly clamped at its edges (see Fig. 8), the relationship between the center displacement  $\delta$  and the load  $P(\delta)$  can be given by Eq. (8).

$$P^* = \begin{cases} 1 + \alpha_1 U + \alpha_2 U^2 & U \leq U^* \\ \beta_1 + \beta_2 U + \beta_3 / U & U > U^* \end{cases} \quad (8)$$

Where

$$\begin{aligned} P^* &: P(\delta)/P_{\ell} & \alpha_1 &= \frac{1 + 2\lambda_n R/\rho}{(2 + \lambda_n R/\rho)(1 + \lambda_n R/\rho)} \\ U &: \delta/t' \\ U^* &: (1 + \lambda_n(R/\rho))/2 & \alpha_2 &= \frac{2(1 + 3\lambda_n R/\rho)}{3(2 + \lambda_n R/\rho)(1 + \lambda_n R/\rho)^2} \\ P(\delta) &: \text{load} \\ P_{\ell} &: \text{limit load} & \beta_1 &= \frac{3 + \lambda_n R/\rho}{2(2 + \lambda_n R/\rho)} \end{aligned}$$



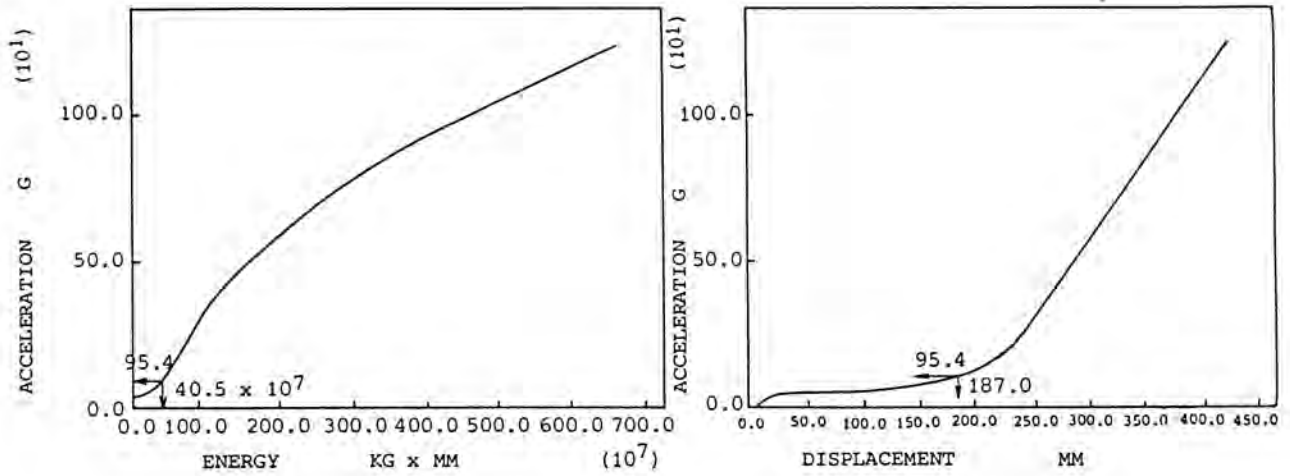


Fig. 6. Output Example of the Evaluation Results by CASH-II Code (Type-II Cask).

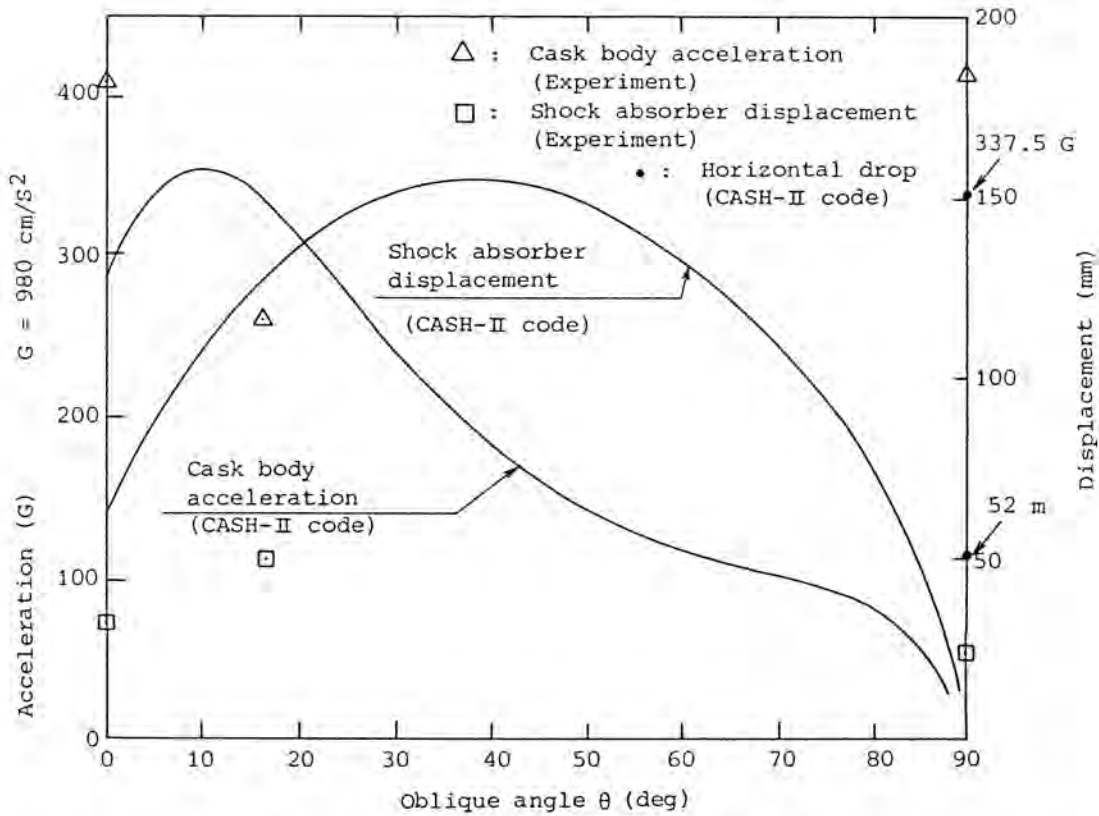


Fig. 7. CASH-II Calculation and Experiment (Displacement vs. Acceleration-Type-I Cask).

TABLE I

Specifications of the Casks Developed by MHI.

	Type I cask	Type II cask	
Cask overall structure			
	Cask weight W (kg)	9600	45000
	Moment of inertia I (kg-mm <sup>2</sup> )	$9.65 \times 10^5$	$3.914 \times 10^6$
	Distance between the center of gravity and the corner $\delta_c$ (mm)	1731	3228
	Corner angle $\theta_c$ (°)	18.3	16.2
Schock absorber model			

TABLE II

Results of CASH-II Code Analyses.

	Oblique Angle $\theta$ (deg)	CASH-II Code		Experiment		Sophisticated Code (PISCES)		Remarks
		Acc. (G)	Dis.(mm)	Acc. (G)	Dis.(mm)	Acc. (G)	Dis.(mm)	
Type I Cask (9600kg)	0	167	63.4	200	50	229	48.0	Full Scale
	18.3	77.3	310.0	49	236	-	-	
	90	125.7	119.8	150	94	-	-	
Type II Cask	0	287.5	62.3	408	29	355	33	1/3 Scale
	16.2	345	127	259	51	-	-	
	90	337.5	52	417	24	-	-	
	0	95.4	187.0	-	-	113.7	133.6	Full Scale
	16.2	111.5	381.0	-	-	-	-	
	90	113.6	139.0	-	-	-	-	

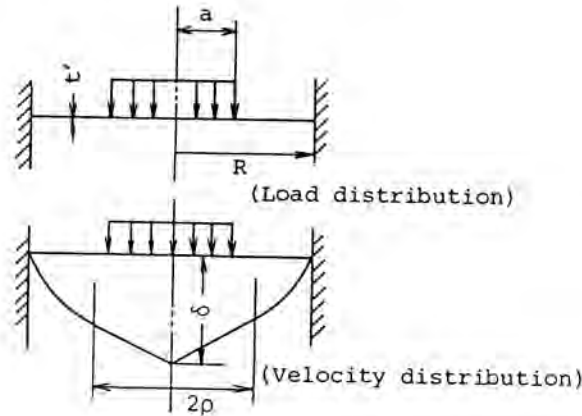


Fig. 8. Analysis Model of a Multilayer Plate with a Distributed Load.

- w : center displacement
- t' : equivalent plate thickness
- R : radius of the plate
- ε : discontinuity radius of the velocity curvature
- a : radius of the loaded area

$$\beta_2 = \frac{2(1 + 2\ln R/\rho)}{(2 + \ln R/\rho)(1 + \ln R/\rho)}$$

$$\beta_3 = \frac{1 + \ln R/\rho}{12(2 + \ln R/\rho)}$$

In converting a three-layer plate into an equivalent single layer plate, the equivalent plate thickness  $t'$  and the equivalent stress  $\sigma_f'$  are related by Eq. (9).

$$\left. \begin{aligned} t' &= 4M_p/N_p \\ \sigma_f' &= N_p/t' \end{aligned} \right\} \quad (9)$$

Where

$M_p$ : Section yield moment of the three-layer plate (per unit width)

$N_p$ : Section yield load of the three-layer plate (per unit width)

On the assumption that plug failures occur in the three layers, the failure load  $P_c$  is given by Eq. (10).

$$P_c \geq \pi d (\tau_1 t_1 + \tau_2 t_2 + \tau_3 t_3) \quad (10)$$

Where

d: Diameter of the mild steel bar

$t_1, t_2, t_3$ : Plate thickness of each layer

$\tau_1, \tau_2, \tau_3$ : Failure shear stress in each layer

Now, the relation between the load  $P_b$  and the displacement  $\delta_b$  of the mild steel bar is assumed to be  $P_b = P_b(\delta_b)$ , in this case, when the cask whose weight is  $W$  is dropped from a height of  $H$  onto the steel bar, the maximum displacement of the cask  $\delta^*$ , that of the bar  $\delta_b^*$  and the maximum acceleration of the cask  $G^*$  are given by the following equations:

$$\begin{aligned} W \cdot H &= \int_0^{\delta^*} P(\delta) d\delta + \int_0^{\delta_b^*} P_b(\delta_b) d\delta_b \\ P(\delta) &= P_b(\delta_b) \\ G^* &= P(\delta^*)/W \end{aligned} \quad (11)$$

If the value of  $P(\delta^*)$  is less than the failure load  $P_c$  given by Eq. (10), the cask is not punctured.

Comparison Between CAPUC Calculation and Experiment

A comparison between the CAPUC code analyses and the LLNL experiments (2) is shown in Table III. Figure 9 gives the relation between the load and displacement for the Run No. ( $d/t_1 = 3$ ) in the Table III.

Comparisons between the CAPUC code analyses and MHI static experiments on a steel plate and a steel-balsa-steel plate are shown in Fig. 10.

As shown above, the CAPUC code analysis results fairly agree with those from the LLNL and MHI experiments performed on single- and multi-layer circular plates, suggesting the CAPUC code can practicably estimate the actual data to be obtained by the 1-m puncture test.



TABLE III

Comparison Between the CAPUC Code and the Experimental Data on Puncture Experiments for Lead-Backed and Edge-Clamped Stainless Steel Plates.

Run No.	Structural Data						Load-Displacement Data					
	Diameter of Bar: d(mm)	Length of Bar: l(mm)	Thickness of stainless steel: t <sub>2</sub> (mm)	Thickness of Lead: t <sub>1</sub> (mm)	Diameter of Plate: D(mm)	d/t <sub>1</sub>	Failure Load (10 <sup>3</sup> kgw)			Puncture Energy (10 <sup>5</sup> kgw-mm)		
							Experiment (Static)	Experiment (Dynamic) (3)	CAPUC(2)	Experiment (Static)	Experiment (Dynamic) (3)	CAPUC(2)
1	15.24	20.32	1.27	15.24	203.2	12.0	3.175	3.856	3.638	0.265	0.288	0.533
2	15.24	20.32	5.08	15.24	203.2	3.0	11.52	12.07	10.40	1.676	1.529	1.718
3	23.77	31.69	8.204	23.77	203.2	2.9	- (1)	31.25	26.08	-	6.636	5.683
4	38.10	50.80	2.972	38.10	203.2	12.8	17.69	20.73	21.84	2.685	2.731	4.879

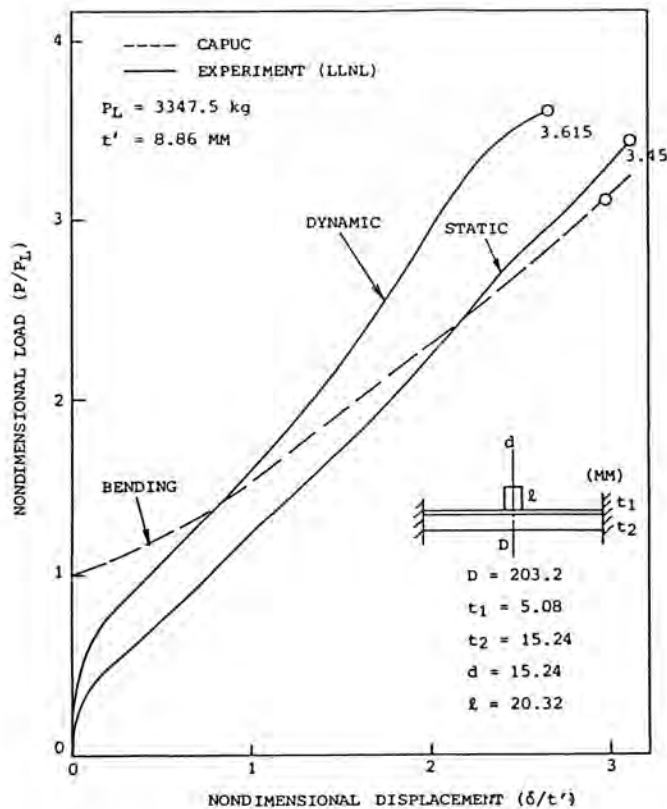


Fig. 9. Load vs. Displacement (LLNL Experiment, Run No. 2).

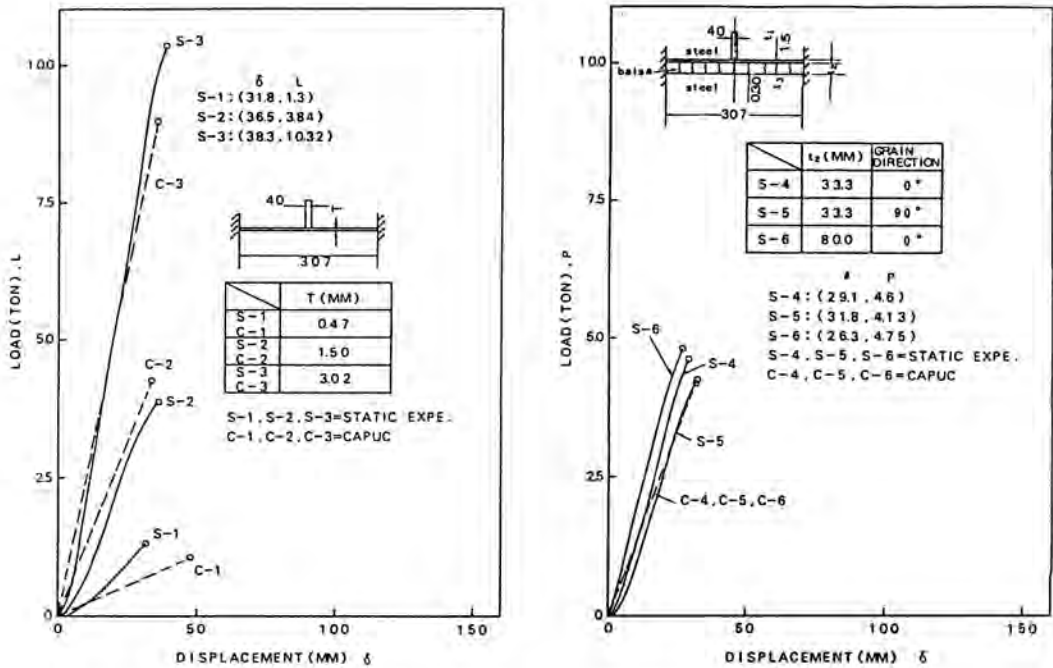


Fig 10. Load vs. Displacement (MHI Experiment).

**CONCLUSION**

In regard to the evaluation of the cask behaviors at the 9-m drop and the 1-m puncture tests, these two codes of CASH-II and CAPUC make the analyses economical by shortening input and calculation times to about 1/50 or less as compared with other codes to analyze dynamic interactions.

The results obtained from these codes have enough accuracy for their practical use, and can be effectively used by multiplying safety (dynamic) factors which have been determined based on the previous extensive experiments and comparative studies with other codes.

As for CASH-II code, it was utilized to get a license of a spent fuel transport cask which has been already in practical use.

These codes are further being utilized satisfactorily in designing not only spent fuel transport casks but also those for fresh fuel transport both of which are under development by MHI.

**REFERENCES**

1. Onat, E. T., and Haythornthwaite, R. M., "The Load-Carrying Capacity of Circular Plates at Large Deflection," ASME Journal of Applied Mechanics, Vol. 23, (1955), pp. 49-55.
2. Larder, R. A., and Arthur, D., "Puncture of Shielded Radioactive Material Shipping Containers, Part-I - Analysis and Results," NUREG/CR-9030, UCRL-52638, Lawrence Livermore Laboratory (1978).